The emergence of classical behaviour in magnetic adatoms

2015 EPL 109 57001

(http://iopscience.iop.org/0295-5075/109/5/57001)

epl A Letters Journal Exploring the Frontiers of Physics

March 2015

EPL, **109** (2015) 57001 www.epljournal.org
doi: 10.1209/0295-5075/109/57001

The emergence of classical behaviour in magnetic adatoms

F. Delgado[1,2,3], S. Loth[4,5], M. Zielinski[6] and J. Fernández-Rossier[1]

[1] *International Iberian Nanotechnology Laboratory (INL) - Av. Mestre José Veiga, P-4715-310 Braga, Portugal*
[2] *Centro de Física de Materiales, CSIC-UPV/EHU - Paseo Manuel de Lardizabal 5, E-20018 San Sebastián, Spain*
[3] *IKERBASQUE, Basque Foundation for Science - E-48013 Bilbao, Spain*
[4] *Max Planck Institute for the Structure and Dynamics of Matter - Hamburg, Germany*
[5] *Max Planck Institute for Solid State Research - Stuttgart, Germany*
[6] *Institute of Physics, Faculty of Physics, Astronomy and Informatics, Nicolaus Copernicus University Grudziadzka 5, PL-87-100 Torun, Poland*

received 10 December 2014; accepted in final form 18 February 2015
published online 9 March 2015

PACS 72.15.Qm – Scattering mechanisms and Kondo effect
PACS 75.78.-n – Magnetization dynamics
PACS 75.10.Jm – Quantized spin models, including quantum spin frustration

Abstract – A wide class of nanomagnets shows striking quantum behaviour, known as quantum spin tunnelling (QST): instead of two degenerate ground states with opposite magnetizations, a bonding-antibonding pair forms, resulting in a splitting of the ground-state doublet with wave functions linear combination of two classically opposite magnetic states, leading to the quenching of their magnetic moment. Here we study how QST is destroyed and classical behaviour emerges in the case of magnetic adatoms, where, contrary to larger nanomagnets, the QST splitting is in some instances bigger than temperature and broadening. We analyze two different mechanisms for the renormalization of the QST splitting: Heisenberg exchange between different atoms, and Kondo exchange interaction with the substrate electrons. Sufficiently strong spin-substrate and spin-spin coupling renormalize the QST splitting to zero allowing the environmental decoherence to eliminate superpositions between classical states, leading to the emergence of spontaneous magnetization. Importantly, we extract the strength of the Kondo exchange for various experiments on individual adatoms and construct a phase diagram for the classical to quantum transition.

Understanding how matter, governed by quantum mechanics at the atomic scale, behaves with classical rules at the macroscale is one of the fundamental open questions in physics [1–3]. One of the most drastic manifestations of the quantum character is found when a system is prepared in a linear combination of two classically different states. In magnetic systems, such a quantum state results in the phenomenon of quantum spin tunnelling (QST) [4], inducing an energy splitting Δ_0 between the two lowest-energy states and quenching their average magnetization.

Attending to the nature of their ground state, nanoscale quantized spin systems can be classified in two groups, see figs. 1(a), (b). Type-C systems, such as single half-integer spins or chains of Ising coupled spins, have two degenerate ground states with wave functions $|C_1\rangle$ and $|C_2\rangle$ that correspond to states with opposite magnetizations. Type-Q systems, such as anisotropic single integer spins, have a unique ground state $|\phi_G\rangle$, as well as a first excited state $|\phi_X\rangle$, both satisfying

$$|\phi\rangle = |C_1\rangle + e^{i\theta}|C_2\rangle, \tag{1}$$

where θ is a phase. Whereas both correspond to quantum spins, only type-Q systems depart radically from the classical picture of a nanomagnet because the quantum expectation value $\langle\phi|\vec{S}|\phi\rangle$ of the atomic spin operator $\vec{S}$ vanishes identically, and not only in the statistical sense. The two degenerate ground states of type-C systems could be prepared in superposition states like (1), but coupling to the environment would rapidly lead to decoherence, restoring the classical behaviour [5]. In contrast, in type-Q systems the coherent superposition emerges dynamically, and it is protected by the energy separation Δ_0 between $|\phi_G\rangle$ and $|\phi_X\rangle$, see fig. 1(b). Examples of type-Q magnets are found in transition metal impurities in insulators [6], spin colour centres [7], magnetic molecules [8] and single molecule-magnets [4].

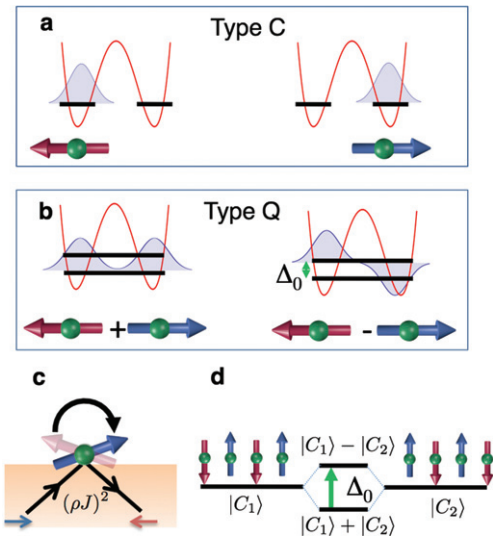

Fig. 1: (Colour on-line) Two types of quantized spin systems. (a) Scheme of a type-C spin system, with an easy axis and two degenerate ground states, bearing each a finite magnetic moment. (b) Type-Q spin system. Due to QST, bonding and antibonding linear combination of states with opposite magnetization, are formed and are separated in energy by Δ_0, the QST splitting. (c) Scheme of Kondo exchange interaction between a single magnetic atom and conduction electrons that quenches Δ_0 (see fig. 2) as (ρJ), the product of the density of states of conducting electrons and the Kondo exchange, is increased. (d) Representation of the two classical degenerate Néel states for spin chains, denoted as $|C_1\rangle$ and $|C_2\rangle$, as well as the type-Q bonding and anti-bonding states and their corresponding QST splitting.

Here we focus on magnetic atoms deposited on conducting surfaces [9–12], where scanning tunnelling microscopes (STM) can probe the two quantities that characterize the quantum or classical behaviour: the quantum spin tunnelling splitting Δ, which can be measured by inelastic electron tunnelling spectroscopy [8,9,11], and the magnetization, accessible through spin-polarized STM [13].

It has been found that diverse magnetic adatoms can be described with the spin Hamiltonian [4,9,11,14]

$$\mathcal{H}_{\rm S} = D\hat{S}_z^2 + E\left(\hat{S}_x^2 - \hat{S}_y^2\right). \qquad (2)$$

This Hamiltonian yields a type-Q spectrum for integer spins ($S = 1, 2, \ldots$) with negative uniaxial anisotropy $D < 0$ and finite in-plane anisotropy E. In that case, both the non-degenerate ground state $|\phi_G\rangle$ and the first excited state $|\phi_X\rangle$, split by $\Delta_0 \propto E(E/D)^{S-1}$, satisfy eq. (1) with $|C_1\rangle \approx |+S\rangle$ and $|C_2\rangle \approx |-S\rangle$ (see fig. 1(a)). This Hamiltonian correctly accounts for the observed dI/dV spectra of Fe adatoms on Cu_2N/Cu(100) [9], Fe Phthalocyanine (FePc) molecules on CuO/Cu(110) [8] and Fe adatoms on InSb [11] (with $S = 2$ for Fe/Cu_2N and $S = 1$ for the others). In these three systems the dI/dV spectra reveal finite quantum spin tunnelling between $|\phi_G\rangle$ and $|\phi_X\rangle$, and a null magnetic moment is expected. One important difference with the case of molecular magnets and magnetic grains [15] is the fact that, for some adatoms, the QST splitting is larger than thermal energy and the reservoir-induced broadening, and it can be larger than the exchange coupling between adatoms.

Moreover, spin-polarized STM magnetometry on short chains of Fe atoms on Cu_2N/Cu(100) is not able [16] to detect finite magnetic moment, consistent with a type-Q behaviour and the observation of QST splitting on the single atom. Intriguingly, longer chains display a spontaneous atomic magnetization, in the form of either antiferromagnetically aligned Néel states [16] or ferromagnetically ordered states [17], depending on orientation of the chain on the surface. In both cases, assembling type-Q atoms on a surface can result in a type-C chain.

The main objective of this work is to model how the QST splitting is renormalized both by Kondo interactions and by exchange coupling between magnetic adatoms. In both cases a sufficiently strong coupling results in the quenching of the QST splitting so that the dressed type-Q system becomes effectively a type C exhibiting two classical degenerate ground states.

We consider first the Kondo exchange in the weak-coupling regime, where the type-Q magnetic adatom spin preserves its identity and the Kondo singlet has not been formed. In that limit, perturbation theory predicts [18] that Kondo exchange produces both a broadening Γ and a shift of the atomic spin excitations [19], in agreement with experiments [20,21]. Both quantities are proportional to the dimensionless constant $(\rho J)^2$, the product of the density of states ρ of the surface electrons and the Kondo exchange J. Here we go beyond perturbation theory and show that a sufficiently large ρJ completely quenches the QST. In the first place, we assume that the separation of the ground-state doublet from the higher excited states is larger than any other relevant energy scale, such as thermal energy or the QST, so that we can truncate the $2S+1$ Hilbert space to only two states, $|\phi_G\rangle$ and $|\phi_X\rangle$. For convenience, we define the Pauli matrices acting on this subspace, denoted by $\vec{\tau}$. Importantly, within the ground-state doublet, the operators S_x and S_y are zero, and only S_z has finite matrix elements that induce transitions between ϕ_G and ϕ_x:

$$J\left(\hat{S}_x, \hat{S}_y, \hat{S}_z\right) \rightarrow j\,(0, 0, \hat{\tau}_x)\,, \qquad (3)$$

where $j \equiv J\langle\phi_G|\hat{S}_z|\phi_X\rangle$. This means that the exchange coupling acts only through the S_z-conserving (Ising) channel, and hence, the Kondo spin-flip terms are totally suppressed within the ground-state doublet. This contrasts with the $S > 1/2$ half integer case, in which the Kondo spin-flip terms are reduced, but not suppressed [22]. Importantly, eq. (3) will equally apply to integer spins with different symmetries, including a cubic environment, as well as systems with an easy axis and in-plane anisotropy with n-fold rotational symmetry [23,24].

As a consequence, the Kondo Hamiltonian projected in the $\{|\phi_G\rangle, |\phi_X\rangle\}$ subspace has the form

$$H_{\rm K} = \frac{\Delta_0}{2}\hat{\tau}_z + \sum_{\vec{k},\sigma} \epsilon_{|\vec{k}|} c^\dagger_{\vec{k},\sigma} c_{\vec{k}\sigma} + \hat{\tau}_x \sum_{\vec{k},\vec{k}'} \frac{j}{2}\left(c^\dagger_{\vec{k},\uparrow} c_{\vec{k}'\uparrow} - c^\dagger_{\vec{k},\downarrow} c_{\vec{k}'\downarrow}\right). \quad (4)$$

This effective Hamiltonian has been used before [25] to describe $J = 4$ spins in URu_2Si_2.

The Kondo-Ising Hamiltonian can be mapped exactly into the spin-boson (SB) model, which permits obtaining rigorous non-perturbative results [26]. In so doing, we assume that the magnetic atom is a a point scatterer. Using the standard partial wave decomposition, only s-wave scattering is possible, which allows treating conduction electrons as one-dimensional fermions for which the bosonization technique [27] can be applied. In this language, the electron-hole excitations across the Fermi energy are represented in terms of bosonic operators $b_k, b_k^\dagger$ [26,28], where $b_k^\dagger$ is a linear combination of states where an electron is promoted from a state below the Fermi surface to another above with additional momentum k. Thus, following a standard calculation [25,26], the Hamiltonian (4) can be written as [15,25,26]

$$H_{SB} = \frac{\Delta_0}{2}\hat{\tau}_z + \sum_{k>0} \epsilon_k b_k^\dagger b_k + \hat{\tau}_x \sqrt{\alpha} \sum_k g_k \left(b_k^\dagger + b_k\right), \quad (5)$$

where the first term describes the QST of the bare magnetic atom, the second electronic excitations of the surface, with $\epsilon_k = \hbar v_F k$, and the third term accounts for the Kondo interaction with $g_k = \hbar v_F (\pi|k|/L)^{1/2} e^{-k v_F/2\omega_c}$, being $\hbar\omega_c$ an energy cutoff and v_F the Fermi velocity.

The SB Hamiltonian is the paradigmatic model to describe the quenching of quantum tunnelling of a two-level system due to its coupling to the environment [26]. All the properties of the model are controlled by the dimensionless parameter α, which in our case is quantifies the strength of the Kondo interaction, $\alpha = (\rho j)^2$. The Kondo-Ising coupling favours localization of the system in one of the two states with $S_z \approx \pm S$ and competes with the QST which favours the mixing of states with opposite S_z. As a result, the QST splitting is renormalized by the Kondo interactions according to [26,29]

$$\frac{\Delta}{\Delta_0} \approx \Theta(1-\alpha)\left(\frac{\Delta_0}{\hbar\omega_c}\right)^{\frac{\alpha}{1-\alpha}}, \quad (6)$$

where Θ is the step function. This zero-temperature non-perturbative result shows that increasing α decreases Δ/Δ_0 exponentially fast, as shown in fig. 2, vanishing completely when $\alpha \geq 1$. This point marks a zero-temperature quantum phase transition beyond which quantum tunnelling is fully suppressed. At finite temperatures, the SB model predicts that spin Rabi oscillations, and therefore the existence of a type-Q non-degenerate ground state, are suppressed when $\Delta/(k_B T) \lesssim 2\alpha$ [26].

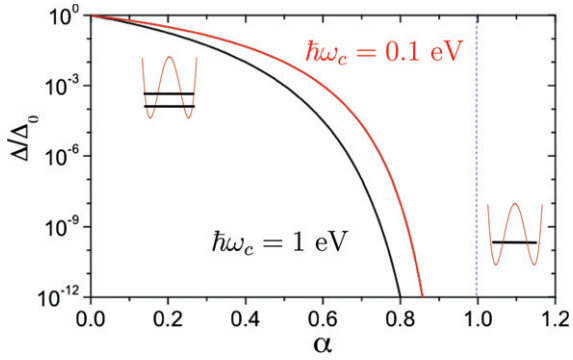

Fig. 2: (Colour on-line) Zero-temperature renormalized splitting Δ in units of the unperturbed level splitting Δ_0, eq. (5), for two different energy cutoffs $\hbar\omega_c = 0.1\,\text{eV}$ (red line) and $1\,\text{eV}$ (black line), both with $\Delta_0 = 1\,\text{meV}$ (notice the logarithmic scale).

Importantly, IETS measures Δ and permits inferring α. The intrinsic line width of a transition between two states 1 and 2 can be extracted from the experiment, removing the trivial effects of thermal smearing and lock-in modulation, and related to α by means of the perturbative result [5]:

$$\Gamma_{2,1} = \alpha \frac{\pi}{2\eta^2} \Delta_{21} \left[1 + n_B(\Delta_{21})\right] \sum_a \left|\langle\phi_1|\hat{S}_a|\phi_2\rangle\right|^2, \quad (7)$$

where $\eta = j/J$, Δ_{21} is the energy of the transition and n_B is the thermal Bose factor. Thus, reading both Δ_{21} and α from the experiments of Fe adatoms on a variety of surfaces, we can place them in a phase diagram, see fig. 3. In the case of Fe on $Cu_2N/Cu(100)$ as well as FePc and Fe on InSb we find that $\alpha \ll 1$, in agreement with the observed finite QST. In the case of Fe atoms on surfaces with C_{3v} symmetry [11,12], the bare QST splitting is zero [23]. However, one can still infer that the strong coupling ($\alpha > 1$) of Fe on Cu(111) would lead to a null QST even if some symmetry breaking takes place.

We now address the emergence of classical behaviour in chains of magnetic adatoms. Two sets of different experiments have shown that sufficiently long chains of $S = 2$ Fe atoms on $Cu_2N/Cu(100)$ exhibit classical behaviour (type C), with either two degenerate Néel states [16] or two ferromagnetic classical states [17], depending on the chain direction over the surface. Therefore, since both the experiments and our previous analysis show that QST splitting of Fe on Cu_2N is robust with respect to the Kondo coupling, it has to be the Fe-Fe exchange that causes a renormalization of the QST splitting and permits the emergence of the magnetic moment. Here we use the following Hamiltonian for a chain of N spins:

$$\mathcal{H} = \sum_{n=1}^{N} \mathcal{H}_{\rm S}(n) + J_{\rm H} \sum_{n=1}^{N-1} \vec{S}(n) \cdot \vec{S}(n+1), \quad (8)$$

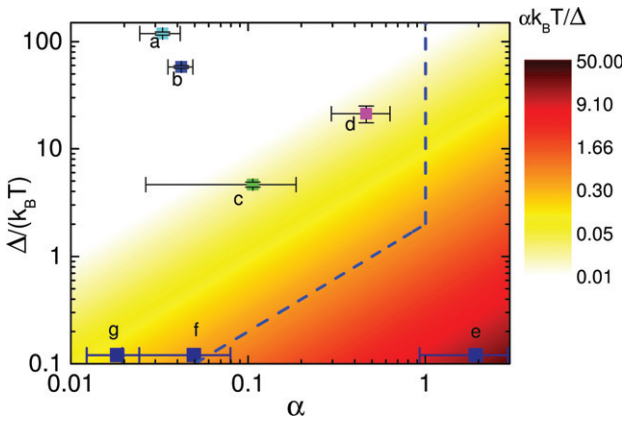

Fig. 3: (Colour on-line) Finite-temperature phase diagram. Axis: renormalized QST splitting Δ/k_BT (vertical), α (horizontal). Quantum region: $\alpha k_BT/\Delta \ll 1$). Classical: ($\alpha k_BT/\Delta \gg 1$). The blue dashed line: quantum to classical boundary ($\alpha = \mathrm{Min}\,[\Delta/(2k_BT), 1]$). Data points: (a), (b) Fe-Phthalocyanine molecules on CuO/Cu(110) [8]; (c) Fe atoms on Cu_2N/Cu(100) [9]; and (d) Fe dopants on InSb(110) [10]. Measured type-C systems, where Δ could not be determined experimentally, are shown over the horizontal axis: (e) Fe atoms on Cu(111) [11], and (g) and (f) Fe atoms on Pt(111) [12].

where the first term describes the $S = 2$ single-ion Hamiltonian of eq. (2) for each Fe, and the second their exchange coupling ($J_H > 0$ for antiferromagnetic (AF) and $J_H < 0$ for ferromagnetic (FM)). Intriguingly, when acting independently, both terms yield a unique ground state without spontaneous magnetization for AF chains. However, their combination gives non-trivial results. This can be first seen using the same truncation scheme of the single-atom case, keeping only 2 levels per site. Hamiltonian (8) then maps into the quantum Ising model with a transverse field (QIMTF):

$$\mathcal{H} \equiv \sum_{n=1}^{N} \frac{\Delta_0}{2}\hat{\tau}_z(n) + j_H \sum_{n=1}^{N-1} \hat{\tau}_x(n)\hat{\tau}_x(n+1), \qquad (9)$$

where $j_H = J_H\,|\langle\phi_G|S_z|\phi_X\rangle|^2$. This model can be solved exactly and presents a quantum phase transition in the thermodynamic limit ($N \to \infty$), separating a type-C from a type-Q phase. In terms of the dimensionless parameter $g \equiv 2|j_H|/\Delta_0$, the transition occurs at $g_c = 1$ [30], see main panel of fig. 4(b). For $g < 1$ the spin chain is in a quantum paramagnetic phase with a unique ground state and $\langle\hat{\tau}_x(n)\rangle = \langle\hat{S}_z(n)\rangle = 0$. For $g \geq 1$, it is in a magnetically ordered phase, with two equivalent ground states with staggered magnetization, $\langle\hat{\tau}_x(n)\rangle \propto \langle\hat{S}_z(n)\rangle \propto (-1)^n$ for the AF chains (and two states with net magnetization for the FM coupling). In this thermodynamic limit, the QST is renormalized by the interactions according to [30]

$$\frac{\Delta}{\Delta_0} = |1-g|\,\Theta(1-g). \qquad (10)$$

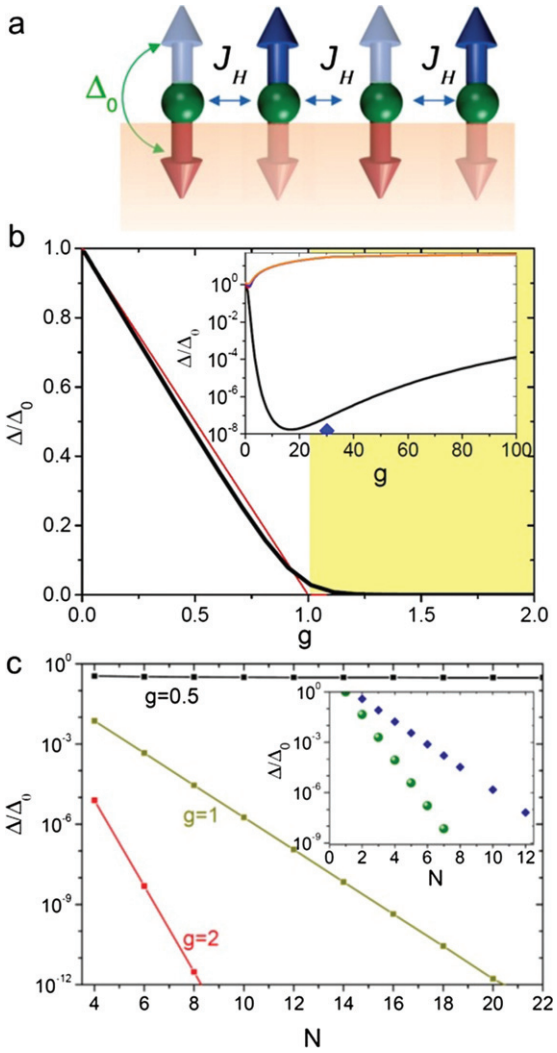

Fig. 4: (Colour on-line) (a) Superposition state of two Néel states. (b) QST splitting of the Ising chain, eq. (8), *vs.* $g = 2|j_H|/\Delta_0$ for a $N = 20$ chain (black line) and the infinite chain (red line, eq. (10)). $g_c = 1$ marks the quantum phase transition. Inset: QST splitting of the $S = 2$ Heisenberg spin chain together with higher-energy excitations (orange lines) *vs.* g for the Fe chains with $D = -1.5\,\mathrm{meV}$ and $E = 0.3\,\mathrm{meV}$ (the diamond marks the experimental condition [16,31] with $g \approx 27$). (c) Chain size dependence of Δ in the QIMTF for $g = 0.5 < g_c$ (weak size dependence), and $g = 1,\ 2$ (exponential dependence that leads to a type-C ground state for large N). Inset: size dependence of Δ for Hamiltonian (8) with the experimental parameters, both for the AF [16,31] and FM chains [17], showing an exponential dependence.

This result shows that, as in the case of Kondo exchange in eq. (6), the interatomic exchange also renormalizes QST, and when sufficiently strong, it suppresses it completely.

Direct application of eqs. (9) and (10) is not possible for the Fe chains on Cu_2N/Cu(100) [16,17,31] where exchange J_H and anisotropy $|D|$ are of the same order, preventing the use of the mapping to an Ising model. Instead, we compute the eigenstates of Hamiltonian (8) numerically,

and compare with those of finite-size chains of the QIMTF (fig. 4), both for FM and AF cases. The small J_H phenomenology is similar to that of the truncated Ising model and the full Heisenberg Hamiltonian: as the Heisenberg interactions are turned on, the QST splitting is reduced (see insets of fig. 4(b) for the AF case). Both the computed ground and first excited states, $|\phi_G\rangle$ and $|\phi_X\rangle$, satisfy eq. (1) with $|C_1\rangle$ and $|C_2\rangle$ being classical Néel-like states for the AF case and fully polarized states with $S_z = \pm 2N$ for the FM case. The next excited states lie much higher in energy.

Crucially, for the experimentally observed values $J_H = 0.7\,\mathrm{meV}$ [16,31] and $J_H = -0.7\,\mathrm{meV}$ [17,31], Δ decreases exponentially with the size of the chain (fig. 4(c)), the effect being much more marked for FM chains. Thus, in this sense we can say that FM coupled chains become classical more easily than AF coupled ones. It has to be noted that the decay of the QST for ferromagnetic is consistent with those of a macro-spin model. In both instances, the results for the full Heisenberg model with single-ion anisotropy are consistent with those of the quantum Ising model in a transverse field. In particular, our numerical results do not show a sign dependence in the weak-coupling regime.

In rigour, interatomic exchange in finite chains renormalizes the QST to a tiny but finite value (see fig. 4). Therefore, the observed [16,17] emergence of classical behaviour is assisted as well by the Kondo coupling. A rigorous direct mapping of the Kondo coupled spin chains to the archetypal spin-boson model of dissipative dynamics is no longer possible. Using results from second-order perturbation theory [5], one finds that the Kondo-induced decoherence rate of a chain of N AF coupled spins is [32]

$$T_2^{-1}(N) = \frac{N\pi}{2}\alpha S^2 \frac{k_B T}{\hbar}. \qquad (11)$$

For instance, the $N = 8$ Fe chain of ref. [16] leads to $\Delta/(\hbar T_2^{-1}) \lesssim 10^{-6}$ at $T = 0.5\,\mathrm{K}$, indicating that the Fe chain will be in the decohered type-C state [5]. Thus, the combination of interatomic exchange, that reduces almost down to zero the QST of the monomer, and the enhanced spin decoherence of the chain due to the Kondo exchange with the substrate, lead to the emergence of the classical behaviour of the finite-size spin chains.

Our results connect the problem of quantum to classical transition in magnetic adatoms with the general ideas established in the 1980s of the role of dissipation in quantum tunnelling [33] and more specifically with the case of molecular magnets and magnetic grains [15]. To the best of our knowledge, the results for the antiferromagnetic chains are very different from any result existing in the literature.

To conclude, a sufficiently strong coupling to either the itinerant electrons or to other localized spins, leads to a phase with a doubly degenerate ground state where classical behaviour appears. Using experimentally verified coupling strengths we find that this transition can occur for small ensembles of interacting atoms ($N < 10$) or even individual atoms. Hence, the classical phase in nanomagnets appears as a quantum phase transition to a quantum decohered phase. Importantly, and in contrast with molecular magnets and magnetic grains, the phase with a QST splitting larger than $k_B T$ is observable, making magnetic adatoms an ideal system to explore the quantum to classical transition experimentally.

* * *

We thank A. J. Heinrich, R. Aguado, M. A. Cazalilla and A. Khajetoorians for fruitful discussions. This work has been financially supported by Generalitat Valenciana, grant Prometeo 2012-11 and Ministerio de Economía y Competitividad, grant FIS2013-47328.

REFERENCES

[1] Anderson P. W., *Science*, **177** (1972) 393.
[2] Zurek W. H., *Phys. Today*, **44**, issue No. 10 (1991) 36.
[3] Zurek W. H., *Rev. Mod. Phys.*, **75** (2003) 715.
[4] Gatteschi D., Sessoli R. and Villain J., *Molecular Nanomagnets* (Oxford University Press, New York) 2006.
[5] Delgado F. and Fernández-Rossier J., *Phys. Rev. Lett.*, **108** (2012) 196602.
[6] Abragam A. and Bleaney B., *Electron Paramagnetic Resonance of Transition Ions* (Oxford University Press, Oxford) 1970.
[7] Childress L., Gurudev Dutt M. V., Taylor J. M., Zibrov A. S., Jelezko F., Wrachtrup J., Hemmer P. R. and Lukin M. D., *Science*, **314** (2006) 281.
[8] Tsukahara N., Noto K., Ohara M., Shiraki S., Takagi N., Takata Y., Miyawaki J., Taguchi M., Chainani A., Shin S. and Kawai M., *Phys. Rev. Lett.*, **102** (2009) 167203.
[9] Hirjibehedin C., Lin C.-Y., Otte A., Ternes M., Lutz C. P., Jones B. A. and Heinrich A. J., *Science*, **317** (2007) 1199.
[10] Khajetoorians A. A., Lounis S., Chilian B., Costa A. T., Zhou L., Mills D. L., Wiebe J. and Wiesendanger R., *Phys. Rev. Lett.*, **106** (2011) 037205.
[11] Khajetoorians A. A., Chilian B., Wiebe J., Schuwalow S., Lechermann F. and Wiesendanger R., *Nature*, **467** (2010) 1084.
[12] Khajetoorians A. A., Schlenk T., Schweflinghaus B., dos Santos Dias M., Steinbrecher M., Bouhassoune M., Lounis S., Wiebe J. and Wiesendanger R., *Phys. Rev. Lett.*, **111** (2013) 157204.
[13] Wiesendanger R., *Rev. Mod. Phys.*, **81** (2009) 1495.
[14] Gruber A., Dräbenstedt A., Tietz C., Fleury L., Wrachtrup J. and Von Borczyskowski C., *Science*, **276** (1997) 2012.
[15] Prokof'ev N. and Stamp P., *J. Low Temp. Phys.*, **104** (1996) 143.
[16] Loth S., Baumann S., Lutz C. P., Eigler D. M. and Heinrich A. J., *Science*, **335** (2012) 196.

[17] Spinelli A., Bryant B., Delgado F., Fernández-Rossier J. and Otte A., *Nat. Mater.*, **13** (2014) 782.
[18] Hurley A., Baadji N. and Sanvito S., *Phys. Rev. B*, **84** (2011) 115435.
[19] Delgado F., Hirjibehedin C. and Fernández-Rossier J., *Surf. Sci.*, **630** (2014) 337.
[20] Oberg J. C., Calvo M. R., Delgado F., Moro-Lagares M., Serrate D., Jacob D., Fernández-Rossier J. and Hirjibehedin C. F., *Nat. Nanotechnol.*, **9** (2014) 64.
[21] Loth S., von Bergmann K., Ternes M., Otte A. F., Lutz C. P. and Heinrich A. J., *Nat. Phys.*, **6** (2010) 340.
[22] Romeike C., Wegewijs M. R., Hofstetter W. and Schoeller H., *Phys. Rev. Lett.*, **96** (2006) 196601.
[23] Miyamachi T., Schuh T., Märkl T., Bresch C., Balashov T., Stöhr A., Karlewski C., André S., Marthaler M., Hoffmann M. *et al.*, *Nature*, **503** (2013) 242.
[24] Hübner C., Baxevanis B., Khajetoorians A. A. and Pfannkuche D., *Phys. Rev. B*, **90** (2014) 155134.
[25] Sikkema A. E., Buyers W. J. L., Affleck I. and Gan J., *Phys. Rev. B*, **54** (1996) 9322.
[26] Leggett A. J., Chakravarty S., Dorsey A. T., Fisher M. P. A., Garg A. and Zwerger W., *Rev. Mod. Phys.*, **59** (1987) 1.
[27] Schotte K. D. and Schotte U., *Phys. Rev.*, **182** (1969) 479.
[28] Mattis D. and Lieb E., *J. Math. Phys.*, **6** (1965) 304.
[29] Hur K., *Ann. Phys.*, **323** (2008) 2208.
[30] Pfeuty P., *Ann. Phys.*, **57** (1970) 79.
[31] Bryant B., Spinelli A., Wagenaar J. J. T., Gerrits M. and Otte A. F., *Phys. Rev. Lett.*, **111** (2013) 127203.
[32] Delgado F. and Fernández-Rossier J., *Kondo exhange induced decoherence in spin chains*, in preparation.
[33] Caldeira A. O. and Leggett A. J., *Phys. Rev. Lett.*, **46** (1981) 211.